Int. J. Electrochem. Sci., 17 **(2022)** Article Number: 220918, doi: 10.20964/2022.09.24

International Journal of
ELECTROCHEMICAL
SCIENCE
www.electrochemsci.org

A Novel Bias Compensated Recursive Least Squares and Multi Innovation Unscented Kalman Filtering Algorithm Method for Accurate State of Charge Estimation of Lithium-ion Batteries

Ke Liu, Shunli Wang[*]*, Chunmei Yu, Chuangshi Qi, Xiao Yang, Jialu Qiao*

School of Information Engineering, Southwest University of Science and Technology, Mianyang 621010, China.
[*]E-mail: 497420789@qq.com

Received: 13 May 2022 / *Accepted:* 27 June 2022 / *Published:* 7 August 2022

The accurate estimation of the state of charge (SOC) of lithium-ion batteries plays an important role in the performance and safety of the battery management system (BMS) of clean-energy vehicles. To improve the accuracy of SOC estimation, in this study, the ternary lithium-ion battery is taken as the research object. With a second-order RC equivalent circuit model, a bias compensated recursive least squares (BCRLS) is constructed for online parameter identification and weakens the influence of uncertain noise. Building on this, the multi-innovation unscented Kalman filter (MIUKF) algorithm is proposed to estimate the SOC of the lithium-ion batteries, which improves the accuracy and stability of the prediction results of high-strength nonlinear lithium-ion battery system. To verify the rationality of the constructed SOC estimation model, the SOC is estimated under different working conditions. The experimental results show that when the system is stable, the error of SOC estimation under HPPC and BBDST working conditions is stably controlled by 1.61% and 1.43% respectively. The results show that the BCRLS-MIUKF can estimate lithium-ion SOC with high precision and strong robustness. The proposed algorithm lays a foundation for the efficient operation of BMS.

Keywords: lithium-ion batteries; bias compensated recursive least squares; multi-innovation unscented Kalman filter; state of charge

1. INTRODUCTION

Under the instruction of energy-saving and emission reduction gathering, the automobile industry began to reform, and electric automobiles became the primary trend of its development [1-3]. Lithium-ion batteries have become an excellent alternative for powering electric automobiles for their advantages such as high-energy density, lightweight, non-memory effect, and steady charging [4-6]. The BMS is an essential component to guarantee the safe, reliable and high-efficiency in the operation of the battery

pack [7, 8]. Therefore, precise observance of battery status, in particular SOC, is a vital concern for battery management systems and offers a foundation for energy and power calculations [9-11]. Being a vital and challenging task in the development of electric automobiles [12, 13], it is of positive significance to study accurate and efficient SOC estimation methods.

The commonly used algorithms for lithium-ion battery SOC estimation include the ampere-hour integration method, neural network method, and filtering algorithm based on an equivalent model [14-16]. The ampere-hour integration method is computationally small and can easily be implemented, but the accuracy of the estimation result is greatly affected by the initial SOC value [17-19], an inaccurate initial value will lead to the gradual accumulation of error over time, resulting in large estimation result error [20, 21]. Neural network algorithm can obtain high estimation accuracy, but the amount of calculation of the algorithm is large, and the accuracy of estimation results depends on whether the training set is reasonable or not [22-24]. For filtering algorithms on the basis of the equivalent model, the commonly used algorithm is the extended Kalman filtering (EKF) [25]. EKF algorithm linearizes the nonlinear system by Taylor expansion and ignoring the high-order term, so the SOC estimation result has non negligible linear error. Compared with EKF, the unscented Kalman filtering (UKF) algorithm can get more accurate estimation result, but it has a hard calculation and the hidden danger of easy divergence of the error covariance matrix. Singular value decomposition unscented Kalman filter (SVD-UKF) algorithm is used for SOC estimation, which reduces the amount of calculation and improves the calculation accuracy. Wei et al. [26] proposed a multi-time scale method for dual estimation of SOC and capacity based on online identification of the battery model to improve the estimation accuracy and stability of the model. Wang et al. [27] explored a multi-model switching estimation algorithm, which can select the most appropriate SOC estimation model online. Hu et al. [28] proposed a co-estimation algorithm for SOC and SOH using a fractional-order model. The model has high estimation accuracy and quick convergence speed due to the closed-loop correction, though the precision of the battery model has a significant impact on the estimation.

For the purpose of representing the SOC of lithium-ion batteries more accurately, based on the construction of a second-order RC model, the BCRLS method is proposed to carry out online parameter identification to weaken the influence of uncertain noise. With the online parameter identification results, the MIUKF algorithm is constructed to realize high-precision SOC estimation. To verify the feasibility of the algorithm, SOC estimation is carried out under the conditions of hybrid pulse power performance experiment (HPPC) and Beijing bus dynamic test (BBDST), and the estimation results are analyzed and compared with different algorithms'.

2. MATHEMATICAL ANALYSIS

2.1. Second-order RC equivalent circuit modeling

A high-precise estimation of SOC is relied on a reasonable selection of battery models, common battery equivalent models include the Rint model, PNGV model, and Thevenin model. Rint model, also known as the internal resistance model, is only composed of one ohmic internal resistance constant voltage source in series. It has low accuracy and linear output and is not suitable for describing the

nonlinear output characteristics of lithium batteries [29]. PNGV model can describe the output characteristics of the battery well , but the series capacitance will increase the cumulative error, and also increase the computational complexity [30]. Thevenin model is also called the first-order RC model. Compared with the first-order RC model, the second-order RC model can better approximate the real battery terminal voltage [31].

This research aims to that the battery model can comprehensively and accurately describe the dynamic characteristics and other electrical characteristics of the battery. On the premise of ensuring accuracy, the amount of calculation should be reduced as much as possible. If the amount of calculation is too large, the model will be very complex and difficult to achieve. Through the analysis and comparison of the above three equivalent circuit models, after comprehensively considering the accuracy, the complexity of parameter identification, and feasibility, a second-order RC equivalent circuit model is established, which is shown in Fig.1.

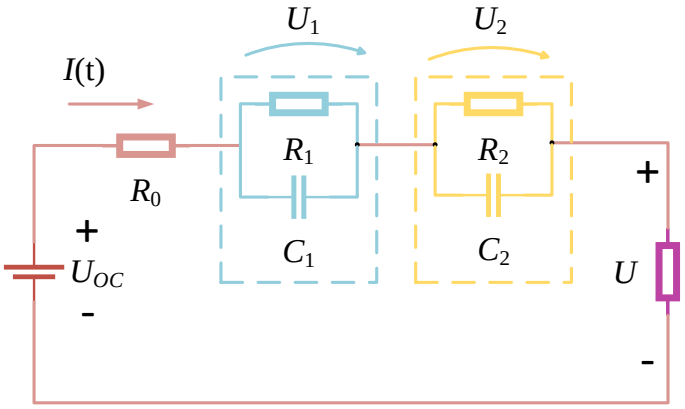

Figure 1. Second-order RC equivalent circuit model

When choosing the second-order RC equivalent circuit model, the equivalent simulation accuracy of electrochemistry of the lithium-ion battery and concentration polarization is higher than that of the first-order RC equivalent circuit model. In accordance with Kirchhoff's law and current law, the equation of state of the model can be gained, in Eq. (1).

$$\begin{cases} U_1 = \dfrac{I}{C_1} - \dfrac{U_1}{R_1 C_1} \\ U_2 = \dfrac{I}{C_2} - \dfrac{U_2}{R_2 C_2} \\ U_{oc} = U + U_1 + U_2 + IR_0 \end{cases} \tag{1}$$

Among them, U_{OC} denotes the open-circuit voltage, U indicates terminal voltage, C_1, C_2 represent electrochemical polarization capacitance and concentration polarization capacitance, respectively, R_1, R_2 represent electrochemical polarization resistance and concentration polarization resistance, respectively, R_0 indicates the ohmic internal resistance of the battery, U_1, U_2 indicate the polarization voltage.

2.2. Online parameter identification based on the BCRLS algorithm

By accurately capturing the real-time characteristics of the system, Recursive Least Squares (RLS) updates the model parameters in real-time based on the current and voltage information collected at the current moment and the state estimation value at the last moment, which can raise the precision of SOC estimation of power cells. From Eq. Eq. (1) the equation of state in the frequency domain can be obtained, as shown in Eq. (2).

$$U_{oc}(s)-U(s)=(R_0+\frac{R_1}{1+R_1C_1s}+\frac{R_2}{1+R_2C_2s})I(s) \tag{2}$$

Let $E(s)=U_{oc}(s)-U(s)$, the transfer function of the system is available to be gained, as shown in Eq. (3).

$$G(s)=\frac{E(s)}{I(s)}=R_0+\frac{R_1}{1+R_1C_1s}+\frac{R_2}{1+R_2C_2s} \tag{3}$$

Eq. (4) can be obtained by bilinear transformation of Eq. (4).

$$\begin{cases} s=\dfrac{2(1-z^{-1})}{T(1+z^{-1})} \\ G(z^{-1})=\dfrac{k_3+k_4z^{-1}+k_5z^{-2}}{1-k_1z^{-1}-k_2z^{-2}} \end{cases} \tag{4}$$

Where, k_1, k_2, k_3, k_4, and k_5 are the constant including the battery model parameters.

From Eq. (4), the standard least square method after discretization can be obtained, as shown in Eq. Eq. (5).

$$\begin{cases} E(k)=\varphi^T(k)\theta(k) \\ \varphi(k)=\left[E(k-1),E(k-2),I(k),I(k-1),I(k-1)\right]^T \\ \theta(k)=\left[k_1,k_2,k_3,k_4,k_5\right]^T \end{cases} \tag{5}$$

In the actual operation of electric automobiles, the acquisition process of the current and voltage of lithium-ion batteries is often accompanied by uncertain noise, which will lead to the deviation of RLS identification results. To improve the ability to the identification of the RLS algorithm, the BCRLS algorithm is used in online parameter identification to attenuate the influence of uncertain noise. The process of improved calculation is shown as follows.

Step 1: Calculate the algorithm gain matrix.

$$K(k)=\frac{P(k-1)\varphi(k)}{1+\varphi^T(k)P(k-1)\varphi(k)} \tag{6}$$

Step 2: Calculate and predict system output and estimated error.

$$e(k)=y(k)-\varphi^{T}(k)\theta_{LS}(k-1) \tag{7}$$

Step 3: Calculate parameter estimation.

$$\theta_{LS}(k)=\theta_{LS}(k-1)-K(k)e(k) \tag{8}$$

Step 4: Calculate the error criterion value.

$$J(k)=J(k-1)+\frac{e^{2}(k)}{1+\varphi^{T}(k)P(k-1)\varphi(k)} \tag{9}$$

Step 5: Update noise variance.

$$\sigma^{2}(k)=\frac{J(k)}{k[1+\theta_{BC}(k-1)D\theta_{LS}(k-1)]} \tag{10}$$

Step 6: Correlation matrix *D*.

$$D=\begin{bmatrix} I_{2\times 2} & 0 \\ 0 & 0_{3\times 3} \end{bmatrix} \tag{11}$$

Step 7: Update the covariance matrix.

$$P(k)=\left[I-K(k)\varphi^{T}(k)\right]P(k-1) \tag{12}$$

Step 8: Estimate the parameters after bias compensation.

$$\theta_{BC}(k)=\theta_{LS}(k)+k\sigma^{2}(k)P(k)D\theta_{BC}(k-1) \tag{13}$$

2.3. Multi innovation unscented Kalman filtering

The unscented Kalman filter uses Kalman linear filter framework to deal with nonlinear problems through unscented transformation to approach the probability distribution of state variables. It has good characteristics of expectations and variance. However, in the process of driving, the working conditions of clean-energy electric vehicles are complex and changeable. To improve the adaptability of UKF in strongly nonlinear systems, the innovation sequence is extended into a multi-dimensional innovation matrix to form a multi-innovation unscented Kalman filter algorithm. By making full use of the measured data information, the accuracy and stability of SOC prediction results are improved.The process of the multi-innovation unscented Kalman filter algorithm is as follows.

Step 1: Set the initial filtering value $\hat{x}_0$ and the square root of the covariance matrix P_0.

$$\begin{cases} \hat{x}_0=E(x_0) \\ P_0=E\left[(x-\hat{x}_0)(x-\hat{x}_0)^{T}\right] \end{cases} \tag{14}$$

Step 2: Calculate Sigma points.

$$\begin{cases} x_{k-1}^{(0)} = \hat{x}_{k-1} \\ x_{k-1}^{(i)} = \hat{x}_{k-1} + \sqrt{n+\lambda} S_{k-1}^{(i)}, i = 1, 2 \cdots n \\ x_{k-1}^{(i)} = \hat{x}_{k-1} - \sqrt{n+\lambda} S_{k-1}^{(i-n)}, i = n+1, n+2 \cdots 2n \end{cases} \tag{15}$$

Step 3: System state variable at time point *k*.

$$\begin{cases} x_{k|k-1}^{(i)} = f(x_{k|k-1}^{(i)}, u_{k-1}) \\ \hat{x}_{k|k-1} = \sum_{i=0}^{2n} w_m^{(i)} x_{k|k-1}^{(i)} \end{cases} \tag{16}$$

Step 4: Calculate the SOC error variance matrix at time point *k*.

$$P_{k,k-1} = \sum_{i=0}^{2n} \omega_c^{(i)} [x_{k|k-1}^{(i)} - \hat{x}_{k|k-1}][x_{k|k-1}^{(i)} - \hat{x}_{k|k-1}]^T + Q_k \tag{17}$$

Step 5: Calculate the battery terminal voltage at time point *k*.

$$\begin{cases} y_{k|k-1}^{(i)} = g(x_{k|k-1}^{(i)}, u_{k-1}) \\ y_{k|k-1} = \sum_{i=0}^{2n} w_m^{(i)} y_{k|k-1}^{(i)} \end{cases} \tag{18}$$

Step 6: Calculate the terminal voltage variance matrix at time point *k*.

$$P_{yy,k} = \sum_{i=0}^{2n} \omega_c^{(i)} [y_{k|k-1}^{(i)} - y_{k|k-1}][y_{k|k-1}^{(i)} - y_{k|k-1}] + R_k \tag{19}$$

Step 7: Calculate the covariance between SOC and measured terminal voltage at time point *k*.

$$P_{xy,k} = \sum_{i=0}^{2n} \omega_c^{(i)} [x_{k|k-1}^{(i)} - \hat{x}_{k|k-1}][x_{k|k-1}^{(i)} - \hat{x}_{k|k-1}]^T \tag{20}$$

Step 8: Calculate the Kalman gain.

$$K_k = \frac{P_{xy,k}}{P_{yy,k}} \tag{21}$$

Step 9: Extend the innovation (e_k) to the innovation matrix ($E_{p,k}$), the Kalman gain (K_k) to the gain matrix ($K_{p,k}$).

$$\begin{cases} e_k = y_k - y_k \\ E_{p,k} = [e_k, e_{k-1}, \cdots, e_{k-p+1}]^T \\ K_{p,k} = [K_k, K_{k-1}, \cdots, K_{k-p+1}] \end{cases} \tag{22}$$

Step 10: Update the modified state update equation.

$$\hat{x}_{k|k} = \hat{x}_{k|k-1} + K_{p,k} E_{p,k} \tag{23}$$

Step 11: Update the error matrix.

$$P_{k|k} = P_{k|k-1} - K_k P_{yy,k} K_k^T \tag{24}$$

2.4. Estimation of SOC by BCRLS-MIUKF algorithm

Combining the BCRLS algorithm with the MIUKF algorithm, a new BCRLS-MIUKF algorithm method for the SOC estimation of lithium-ion batteries is proposed. With $[SOC_k, U_{1,k}, U_{2,k}]^T$ as the state variable and end voltage U_L as the observation variable, the equivalent circuit is discretized and the battery state-space expression is established, as shown in Eq. (25).

$$\begin{cases} \begin{bmatrix} SOC_{k+1} \\ U_{1,k+1} \\ U_{2,k+1} \end{bmatrix} = \begin{bmatrix} 1 & 0 & 0 \\ 0 & e^{\frac{\Delta t}{t_1}} & 0 \\ 0 & 0 & e^{\frac{\Delta t}{t_2}} \end{bmatrix} \begin{bmatrix} SOC_k \\ U_{1,k} \\ U_{2,k} \end{bmatrix} + \begin{bmatrix} -\dfrac{\eta \Delta t}{Q_N} & R_1\left(1-e^{\frac{T}{T_1}}\right) & R_2\left(1-e^{\frac{T}{T_2}}\right) \end{bmatrix}^T I_k + w_k \\ U_{L,k+1} = \begin{bmatrix} \dfrac{\partial U_{oc}}{\partial SOC} & -1 & -1 \end{bmatrix} \begin{bmatrix} SOC_k \\ U_{1,k} \\ U_{2,k} \end{bmatrix} - I_k R_0 + v_k \end{cases} \tag{25}$$

In Eq. (25), T represents the time constant, $T_1=R_1C_1$, $T_2=R_2C_2$; Δt represents sampling interval time. With the discharging direction as positive, I_k means the current at time point k, w_k indicates process noise, v_k stands for measurement noise, and Q_N represents the rated battery capacity. The specific implementation process of joint estimation SOC is shown in Fig. 2.

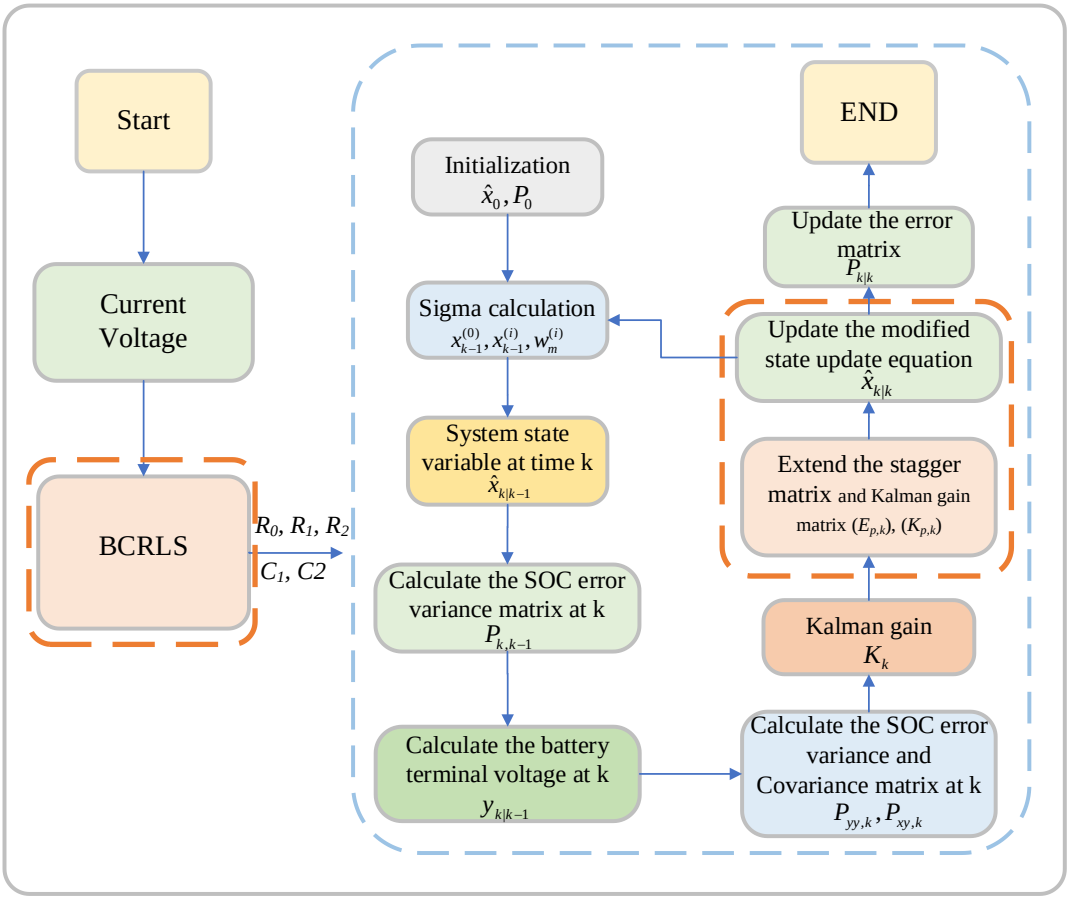

Figure 2. The flow chart of the BCRLS-MIUKF algorithm

3. EXPERIMENTAL ANALYSIS

In accordance with the above steps, the model parameters of the ternary lithium-ion battery are updated in real-time by the BCRLS algorithm, as well as the identification results are provided to the MIUKF algorithm for estimating battery SOC. For verifying the feasibility of the BCRLS-MIUKF algorithm, a lithium battery SOC estimation model is constructed, and the estimation accuracy of the model, convergence from the estimation process, and follow-up on real data real data are verified under HPPC and BBDST working conditions.

3.1. Test platform construction

To verify online parameter identification and MIUKF algorithm through BCRLS, this study adopts a ternary lithium-ion battery with a standard capacity of 70Ah as the research object and adopts BTS200-100-104 battery test equipment as the test platform. The experiment in this study was carried out at a constant temperature of 35°C, and the influence of battery aging on experimental test results was ignored.

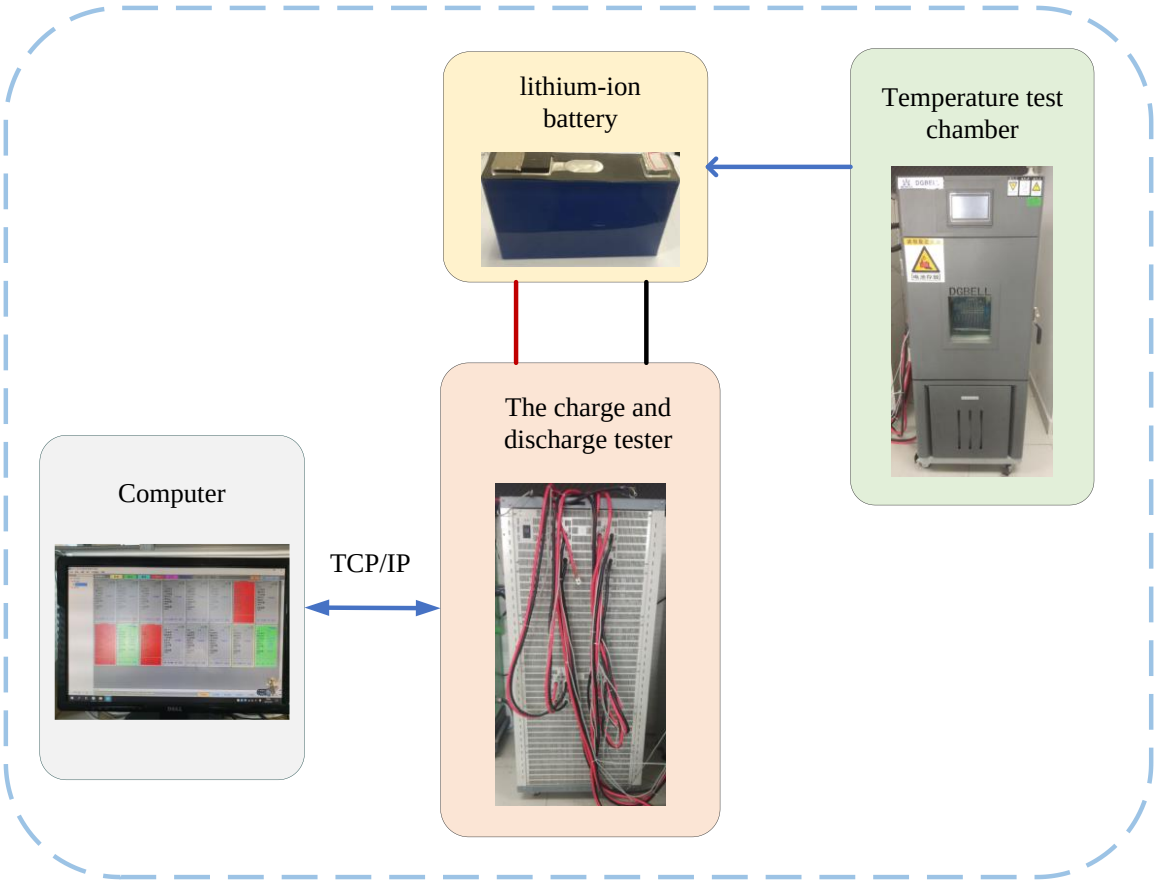

Figure 3. Schematic of the experimental setup

3.2. Online parameter identification experiments based on BCRLS

In consideration of the fact that the battery is usually working in an intermittent discharge state in actual use, and the HPPC working condition includes the state of shelving, charging, and discharging, which conforms to the actual working state of the battery, the proposed BCRLS is validated under the HPPC experimental conditions, and the verification results are provided in Fig. 4.

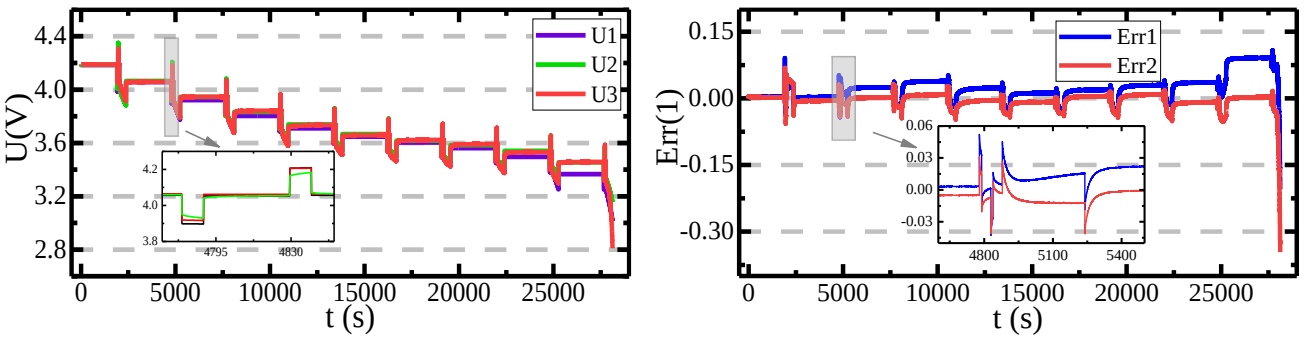

(a) Output comparison (b) output error

Figure 4. Comparison of terminal voltage output curves

Based on the second-order RC equivalent circuit model, Reference [32] adaptive an genetic algorithm (GA) to identify relevant battery parameters, and the average error of voltage is 0.78%; Reference [33] uses the least square method to identify the model parameters, and the average error of voltage estimated by the method is within 0.51%. Reference [34] proposes a method of the Extended Kalman filtering algorithm to identify the model parameters, and the maximum error estimated by the method is within 5%. The figure 4 (a) represents the voltage comparison of RLS and BCRLS parameter identification results, where *U*1 represents the analog voltage corresponding to the RLS algorithm and *U*2 represents the analog voltage corresponding to the BCRLS algorithm. In figure 4 (b), Err1 and Err2 represent the voltage error curves corresponding to RLS and BCRLS, respectively. Through the improvement of the algorithm, the average error of voltage changes from 2.66% to 0.98%. The results of experiments demonstrate that the BCRLS algorithm can effectively decrease the influence of noise on parameter identification and acquire online parameter identification results with high precision, which can be used in follow-up SOC estimation.

3.3. Experimental verification under HPPC working conditions

For verifying the effectiveness and rationality of BCRLS-MIUKF algorithm for lithium-ion batteries SOC estimation under complex application conditions, the HPPC condition is selected for experimental verification. HPPC working condition includes charging, discharging, and shelving processes of different time lengths and simulates the intermittent cycle charging and discharging condition of lithium-ion battery in actual working time.

Setting the actual initial SOC value as 1, and the initial SOC values of other algorithms are 0.8. The SOC estimation results of different algorithms under HPPC working conditions are shown in Fig. 5.

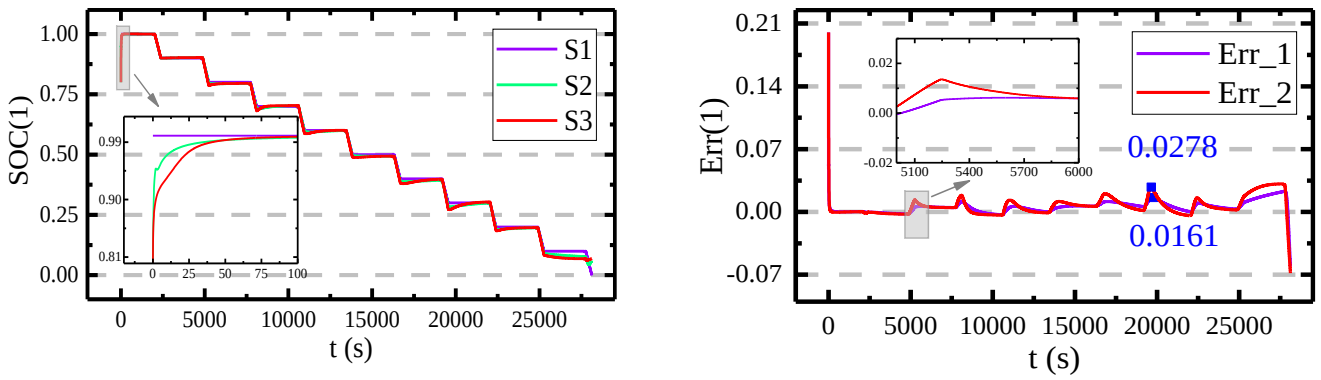

(a) SOC estimation based on BCRLS-MIUKF (b) Error of SOC estimation of BCRLS-MIUKF

Figure 5. BCRLS-MIUKF result curves under HPPC working condition

The figure 5(a) shows the SOC estimation result and figure 5(b) means the error of SOC estimation. It is observed that *S*1 represents the actual SOC result, *S*2 represents the SOC estimation

result of the BCRLS-MIUKF algorithm, *S*3 represents the SOC estimation result of the BCRLS-UKF algorithm, and Err1 and Err2 represent the estimation errors corresponding to *S*2 and *S*3, respectively. It can be seen in figure 5(a), when the initial SOC value of the algorithm is set to 0.8, the convergence speed of the BCRLS-MIUKF algorithm is more rapid than the BCRLS-UKF algorithm. From Figure 5(b), the maximum error of the BCRLS-MIUKF algorithm is 1.61% whereas the maximum error of the BCRLS-UKF algorithm is 2.78%. The results suggest, that the estimation results of the BCRLS-MIUKF algorithm are more accurate considerably.

In this section, the average absolute value error (MAE) and root mean square error (RMSE) of SOC estimation results are used to compare different algorithms, and the results are shown in Table 1.

Table 1. Comparison of SOC estimation results of different algorithms under HPPC working conditions

algorithms	MAE	RMSE
BCRLS-UKF	0.81%	1.26%
BCRLS-MIUKF	0.63%	0.86%

3.4. Experimental verification under BBDST working condition

In practical applications, to further validate the BCRLS-MIUKF algorithm for estimating the SOC of lithium-ion batteries under more conditions of complex applications, the BBDST condition is used for experimental verification. BBDST working condition includes the data of buses in starting, taxiing, acceleration, rapid acceleration, and other operations, which cando a better imitation of the actual situation of lithium-ion batteries in clean-energy vehicles.

Setting the actual initial SOC value as 1, and the initial SOC values of other algorithms are 0.6. The SOC estimation results of different algorithms under BBDST working conditions are displayed in Fig. 6.

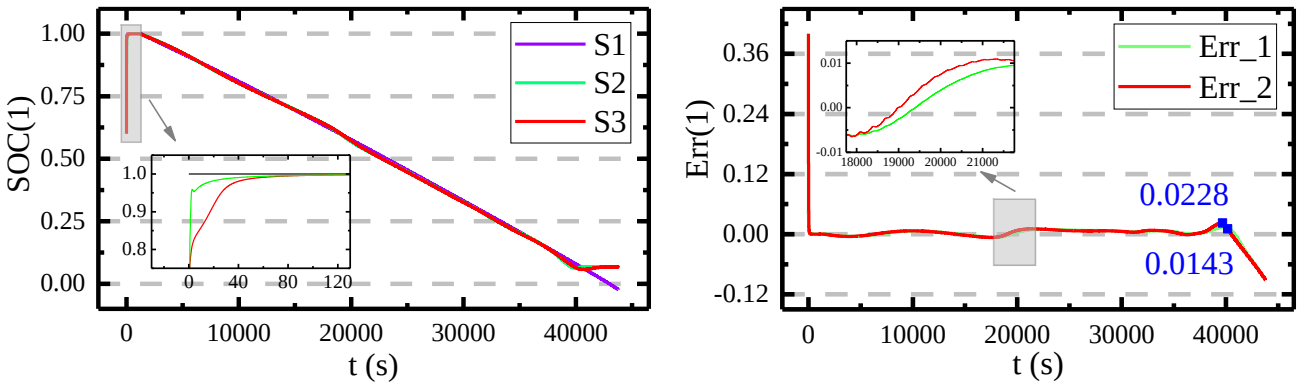

(a) SOC estimation based on BCRLS-MIUKF (b) Error of SOC estimation of BCRLS-MIUKF

Figure 6. BCRLS-MIUKF result curves under BBDST working condition

The figure 6(a) shows the SOC estimation result and figure 6(b) indicates the error of SOC estimation. In Fig. 6, *S*1 denotes the actual SOC result, *S*2 stands for the SOC estimation result of the

BCRLS-MIUKF algorithm, *S*3 represents the SOC estimation result of the BCRLS-UKF algorithm, and Err1 and Err2 denote the estimation errors corresponding to *S*2 and *S*3, separately. From Figure 6(a), it can be seen that, when the SOC value of the algorithm is set to 0.6, the BCRLS-MIUKF algorithm converges faster than the BCRLS-UKF algorithm. From figure 6(b), under BBDST working conditions, in the stable discharge phase, the estimated precision of SOC is the same for both improved algorithms. The estimation effect is not ideal due to the violent internal chemical reaction at the end of battery discharge, but it does not affect the overall estimation effect. In this regard, the maximum error of the BCRLS-MIUKF algorithm is 1.43% while the maximum error of the BCRLS-UKF algorithm is 2.28%. The results also suggest that the BCRLS-MIUKF algorithm possesses more rapid convergence, higher precision, and better estimation under the complex working conditions of BBDST.

Throughout this section, the MAE and RMSE of SOC estimation results are employed to compare different algorithms. The results are shown in Table 2.

Table 2. Comparison of SOC estimation results of different algorithms under BBDST working conditions

algorithms	MAE	RMSE
BCRLS-UKF	0.85%	1.60%
BCRLS-MIUKF	0.79%	1.51%

4. CONCLUSIONS

SOC estimation of Lithium-ion batteries is an important issue and challenge for battery management systems. Then, to obtain high-precision SOC estimation results, based on the second-order RC model, a BCRLS algorithm is proposed, which adds a bias compensation term to the original algorithm to weaken the influence of uncertain noise signals. In addition, a MIUKF algorithm is proposed, which extends the multi-innovation to the innovation matrix. By repeatedly using the data and innovation, it is helpful to improve the error correction effect. This proposed BCRLS-MIUKF joint estimation algorithm is verified through HPPC and BBDST working conditions. The verification results stands for the parameter identification results of the BCRLS algorithm are better than the RLS algorithm. Meanwhile, under HPPC conditions, the maximum error of SOC value estimated by BCRLS-MIUKF is 0.0117 less than BCRLS-UKF. But under BBDST conditions, it is 0.0085. The parameter identification result of the BCRLS algorithm is more accurate than the traditional RLS algorithm. On this basis, the convergence and accuracy of the BCRLS-MIUKF algorithm are better than the BCRLS-UKF algorithm. Therefore, this method has positive implications for the applicability and extension of lithium-ion batteries by providing a basis for optimizing SOC estimation.

ACKNOWLEDGEMENTS
The work is supported by the National Natural Science Foundation of China (No. 62173281, 61801407).

References

1. L. Su, G. Zhou, D. Hu, Y. Liu and Y. Zhu, *Energies*, 14 (2021) 190.
2. X. Yang, S. Wang, W. Xu, J. Qiao, C. Yu and C. Fernandez, *International Journal of Circuit Theory and Applications*, 50 (2022) 614.
3. J. C. A. Anton, P. J. G. Nieto, C. B. Viejo and J. A. V. Vilan, *Ieee Transactions on Power Electronics*, 28 (2013) 5919.
4. Y. Luo, P. Qi, Y. Kan, J. Huang, H. Huang, J. Luo, J. Wang, Y. Wei, R. Xiao and S. Zhao, *International Journal of Energy Research*, 44 (2020) 10538.
5. D. Ge, Z. Zhang, X. Kong and Z. Wan, *Applied Sciences-Basel*, 11 (2021) 220.
6. N. Tian, H. Fang, J. Chen and Y. Wang, *Ieee Transactions on Control Systems Technology*, 29 (2021) 370.
7. X. Liu, X. Deng, Y. He, X. Zheng and G. Zeng, *Energies*, 13 (2020) 1337.
8. J. Qiao, S. Wang, C. Yu, W. Shi and C. Fernandez, *International Journal of Circuit Theory and Applications*, 49 (2021) 3879.
9. P. Xu, B. Liu, X. Hu, T. Ouyang and N. Chen, *Ieee Transactions on Industrial Electronics*, 69 (2022) 6635.
10. T. Ouyang, P. Xu, J. Chen, J. Lu and N. Chen, *Electrochimica Acta*, 353 (2020) 2464.
11. D.-J. Xuan, Z. Shi, J. Chen, C. Zhang and Y.-X. Wang, *Journal of Cleaner Production*, 252 (2020) 237.
12. T. Mamo and F.-K. Wang, *Ieee Access*, 8 (2020) 94140.
13. W. Liu, H. Zhou, Z. Tang and T. Wang, *Journal of Electrochemical Energy Conversion and Storage*, 19 (2022) 797.
14. W. Zhang, L. Wang, L. Wang, C. Liao and Y. Zhang, *Ieee Transactions on Industrial Electronics*, 69 (2022) 3677.
15. P. Qin, Y. Che, H. Li, Y. Cai and M. Jiang, *Journal of Power Electronics*, 22 (2022) 490.
16. X. Y. Lin, Y. L. Tang, J. Ren and Y. M. Wei, *Journal of Energy Storage*, 41 (2021) 538.
17. W. Gao, L. Yan and D. Sun, *Journal of Shanghai University. Natural Science Edition*, 26 (2020) 413.
18. W. Hu, Q. Shang, X. Bian and R. Zhu, *International Journal of Low-Carbon Technologies*, 17 (2022) 169.
19. C. Jiang, S. L. Wang, B. Wu, C. Fernandez, X. Xiong and J. Coffie-Ken, *Energy*, 219 (2021) 2355.
20. M. Adaikkappan and N. Sathiyamoorthy, *International Journal of Energy Research*, 46 (2022) 2141.
21. X. Chen, Z. Gao, R. Ma and X. Huang, *Transactions of the Institute of Measurement and Control*, 42 (2020) 1618.
22. Y. Shen, *Electrochimica Acta*, 336 (2020) 3788.
23. Z. W. Deng, X. S. Hu, X. K. Lin, Y. H. Che, L. Xu and W. C. Guo, *Energy*, 205 (2020) 1687.
24. W. Diao, B. Xu and M. Pecht, *Journal of Power Sources*, 484 (2021) 7893.
25. M. Al-Gabalawy, N. S. Hosny, J. A. Dawson and A. I. Omar, *International Journal of Energy Research*, 45 (2021) 6708.
26. Z. Wei, J. Zhao, D. Ji and K. J. Tseng, *Applied Energy*, 204 (2017) 1264.
27. Y. Wang, C. Zhang and Z. Chen, *Applied Energy*, 137 (2015) 427.
28. M. Hu, Y. Li, S. Li, C. Fu, D. Qin and Z. Li, *Energy*, 165 (2018) 153.
29. M. Wu, L. Qin and G. Wu, *Journal of Energy Storage*, 51 (2022) 266.
30. Y. Geng, H. Pang and X. Liu, *Journal of Power Electronics*, (2022) 789.
31. J. Feng, F. Cai, J. Yang, S. Wang and K. Huang, *Ieee Access*, 10 (2022) 44549.
32. C. Fang, Z. Jin, J. Wu and C. Liu, *Frontiers in Energy Research*, 9 (2021) 556.
33. J. Lv, B. Jiang, X. Wang, Y. Liu and Y. Fu, *Electronics*, 9 (2020) 26.

34. F. Guo, G. Hu, S. Xiang, P. Zhou, R. Hong and N. Xiong, *Energy*, 178 (2019) 79.

© 2022 The Authors. Published by ESG (www.electrochemsci.org). This article is an open access article distributed under the terms and conditions of the Creative Commons Attribution license (http://creativecommons.org/licenses/by/4.0/).